Knee Surgery, Sports Traumatology, Arthroscopy (2021) 29:1164–1172
https://doi.org/10.1007/s00167-020-06122-1

KNEE

Anterior cruciate ligament bundle insertions vary between ACL-rupture and non-injured knees

Dimitris Dimitriou[2] · Diyang Zou[1,3] · Zhongzheng Wang[1,3] · Naeder Helmy[2] · Tsung-Yuan Tsai[1,3]

Received: 12 February 2020 / Accepted: 24 June 2020 / Published online: 1 July 2020

Abstract

Purpose The present study aimed to investigate the three-dimensional topographic anatomy of the anterior cruciate ligament (ACL) bundle attachment in both ACL-rupture and ACL-intact patients who suffered a noncontact knee injury and identify potential differences.

Methods Magnetic resonance images of 90 ACL-rupture knees and 90 matched ACL-intact knees, who suffered a noncontact knee injury, were used to create 3D ACL insertion models.

Results In the ACL-rupture knees, the femoral origin of the anteromedial (AM) bundle was 24.5 ± 9.0% posterior and 45.5 ± 10.5% proximal to the flexion–extension axis (FEA), whereas the posterolateral (PL) bundle origin was 35.5 ± 12.5% posterior and 22.4 ± 10.3% distal to the FEA. In ACL-rupture knees, the tibial insertion of the AM-bundle was 34.3 ± 4.6% of the tibial plateau depth and 50.7 ± 3.5% of the tibial plateau width, whereas the PL-bundle insertion was 47.5 ± 4.1% of the tibial plateau depth and 56.9 ± 3.4% of the tibial plateau width. In ACL-intact knees, the origin of the AM-bundle was 17.5 ± 9.1% posterior ($p < 0.01$) and 42.3 ± 10.5% proximal (*n.s.*) to the FEA, whereas the PL-bundle origin was 32.1 ± 11.1% posterior (*n.s.*) and 16.3 ± 9.4% distal ($p < 0.01$) to the FEA. In ACL-intact knees, the insertion of the AM-bundle was 34.4 ± 6.6% of the tibial plateau depth (*n.s.*) and 48.1 ± 4.6% of the tibial plateau width (*n.s.*), whereas the PL-bundle insertion was 42.7 ± 5.4% of the tibial plateau depth ($p < 0.01$) and 57.1 ± 4.8% of the tibial plateau width (*n.s.*).

Conclusion The current study revealed variations in the three-dimensional topographic anatomy of the native ACL between ACL-rupture and ACL-intact knees, which might help surgeons who perform anatomical double-bundle reconstruction surgery.

Level of evidence III.

Keywords Anterior cruciate ligament · Anteromedial bundle · Posterolateral bundle · Tibial insertion · Double-bundle reconstruction · Tibial footprint · Double-bundle · Femoral origin

Introduction

Over the past years, there has been increasing interest regarding the "anatomical" anterior cruciate ligament (ACL) reconstruction, as this approach has demonstrated higher biomechanical stability and better clinical outcomes than the non-anatomical, transtibial approach [17, 19]. Recently, anatomical double-bundle reconstruction has gained popularity, as several biomechanical studies have reported that it restores more closely the healthy knee kinematics [28, 39, 40], and clinical studies have demonstrated superior outcomes regarding knee laxity and graft failure compared with the single-bundle reconstruction [14, 26, 34].

Multiple anatomical differences of the tibiofemoral joint between ACL-rupture and healthy knees, such as the femoral

Dimitris Dimitriou and Diyang Zou have contributed equally to this article.

✉ Tsung-Yuan Tsai
tytsai@sjtu.edu.cn

1 Shanghai Key Laboratory of Orthopaedic Implants and Clinical Translational R&D Center of 3D Printing Technology, Department of Orthopaedic Surgery, Shanghai Ninth People's Hospital, Shanghai Jiao Tong University School of Medicine; School of Biomedical Engineering and Med.X Research Institute, Shanghai Jiao Tong University, Shanghai 200030, China

2 Department of Orthopedics, Bürgerspital Solothurn, Schöngrünstrasse 42, Solothurn 4500, Switzerland

3 Engineering Research Center of Digital Medicine and Clinical Translation, Ministry of Education, 200030 Shanghai, China

intercondylar notch size [27, 31, 38], lateral femoral condyle ratio [29] and index [11], tibial plateau slope [33] and concavity [2, 24] and tibial eminence morphology [32] have been reported in the literature. Recently, the femoral ACL-footprint origin, as a single bundle, was identified as a possible predisposing factor for ACL injury, as significant differences were observed between ACL-rupture and ACL-intact knees [8]. Despite these well-documented morphological differences between ACL-rupture and healthy knees, the current recommendations for the anatomical double-bundle ACL reconstruction are mostly based on cadaveric studies, performed in ACL-intact knees [5, 6, 10, 13, 15]. An anatomical double-bundle ACL reconstruction requires detailed knowledge of the anteromedial (AM) and posterolateral (PL) bundle anatomy in ACL-rupture patients, as potential differences might exist between ACL-rupture and healthy knees.

The hypothesis of this study was that AM and PL-bundle attachment would be significantly different between ACL-rupture and ACL-intact knees. Therefore, the purpose of the present study was to investigate the three-dimensional, topographic anatomy of the ACL bundle attachment in both ACL-rupture and ACL-intact patients who suffered a non-contact knee injury and identify potential differences.

Materials and methods

Study design and patient selection

The present single-center, retrospective study was approved by the authors' institutional Internal Review Board and the ethical committee (Ethical Committee Northeast and Central Switzerland 2018-01410). All patients who presented in the outpatient clinic with an ACL injury following an acute noncontact knee injury were considered potential candidates for the study. Following receipt of written informed consent, the medical records and magnetic resonance images (MRIs) of all patients (647 patients) from January 2015 to December 2017 were retrospectively reviewed. The exclusion criteria were age > 45 years, history of patellofemoral instability, previous surgery or symptoms in the affected knee, and ACL-rupture following a contact knee injury, as under an adequate amount of energy, the ACL could also rupture in individuals without a predisposition. Ninety ACL-rupture patients (male: 55, female: 35) with a median age of 31 (range 16–45) years were identified. The ACL-rupture patients were then randomly matched for sex, age, and body mass index (BMI) with patients who presented in outpatient clinic following an acute, noncontact knee injury, without an ACL-rupture, that resulted in a bone bruise of the femur or tibia visible on MRI (control group), suggesting an adequate trauma. Ninety patients were identified for inclusion in the control group. The MRIs were reviewed by a senior orthopedic surgeon and a musculoskeletal radiologist to determine concomitant injuries. The exclusion criteria were a history of patellofemoral instability and previous surgery or symptoms in the affected knee.

MRI characteristics and image processing

All the patients were scanned using a 3.0-T MR Scanner (Achieva; Philips Healthcare, The Netherlands). Proton density-weighted turbo spin-echo SPectral Attenuated Inversion Recovery (PDW TSE SPAIR) sagittal-plane images (slice thickness: 1 mm, voxel size: 3.29 by 0.22 by 0.22 mm) and T1 high-resolution turbo spin-echo (T1 HR TSE) coronal-plane images (slice thickness 1 mm, voxel size 0.12 by 2.74 by 0.12 mm) were obtained. The two MR image stacks were combined to yield volumetric data with a voxel size of 0.22 by 0.25 by 0.24 mm (Fig. 1a) using commercial software (AMIRA 6.5, FEI SVG, Thermo Fisher Scientific, Hillsboro, Oregon, USA). Using the same software, the three-dimensional (3D) surface of the distal femur and proximal tibia with its articular cartilage was reconstructed according to a previously validated and published method [7]. The AM and PL-bundles were identified on MRI, according to the Cohen et al. [4] methodology. Briefly, the AM-bundle was defined as the oblique fibers inserting at the anterior border of the ACL on the tibia and the proximal aspect of the femoral insertion on the lateral femoral condyle. Similarly, the PL-bundle was defined as the oblique fibers inserting posteriorly on the tibial insertion and the distal aspect of the femoral insertion on the lateral femoral condyle. Subsequently, the femoral origin and tibial insertion areas of the AM and PL-bundles were digitized, and their centers were calculated (Figs. 1, 2). Finally, the surface models were imported to a self-developed MATLAB (MathWorks, Natick, Massachusetts, USA) script for subsequent analyses.

Anatomical coordinate system of the distal femur and proximal tibia

The anatomical coordinate system of the distal femur (fACS) was reconstructed following the recommendations of Miranda et al. [25]. Briefly, two spheres were best fitted to the posterior articular surface of the medial and lateral condyles using a Gauss–Newton nonlinear least square algorithm (Fig. 1b). The radius of the best-fitted sphere on the lateral femoral condyle was defined as the *lateral femoral condyle width*. The line connecting the centers of the best-fitted spheres formed the *mediolateral* (*M/L*) axis of the fACS and the *flexion–extension axis* (FEA) of the knee, as several studies concluded that the cylindrical axis is coincident with the FEA of the knee [9, 12]. The *lateral femoral condyle width* was used to normalize the femoral ACL-footprint location relative to FEA on the lateral view.

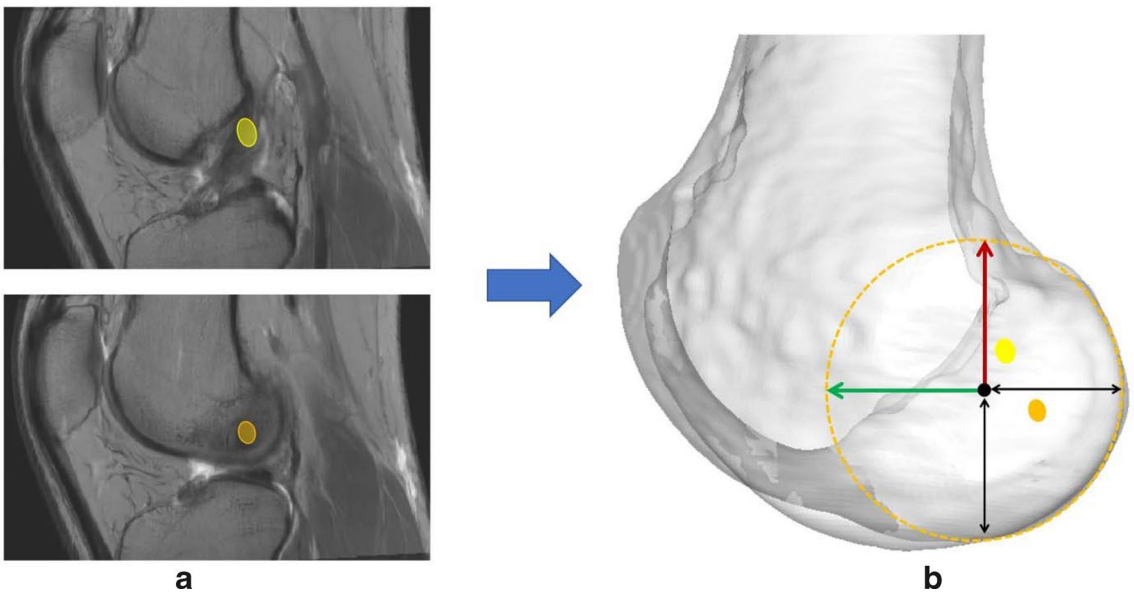

Fig. 1 Left knee with an intact ACL demonstrating the origin of the ACL-bundle origin. **a** High-resolution volumetric MR data were created after merging sagittal and coronal MR stacks. The femoral origin of the AM and PL-bundles is marked with a yellow and orange ellipses, respectively. **b** Three-dimensional surface models of the distal femur with an anatomical coordinate system were constructed. The origin of the coordinate system is shown with a black circle; the proximal/distal axis is demonstrated with a red arrow, whereas the anterior/posterior axis has a green arrow. The lateral femoral condyle width defined as the radius of the best-fitted sphere in the lateral condyle is shown with a black arrow

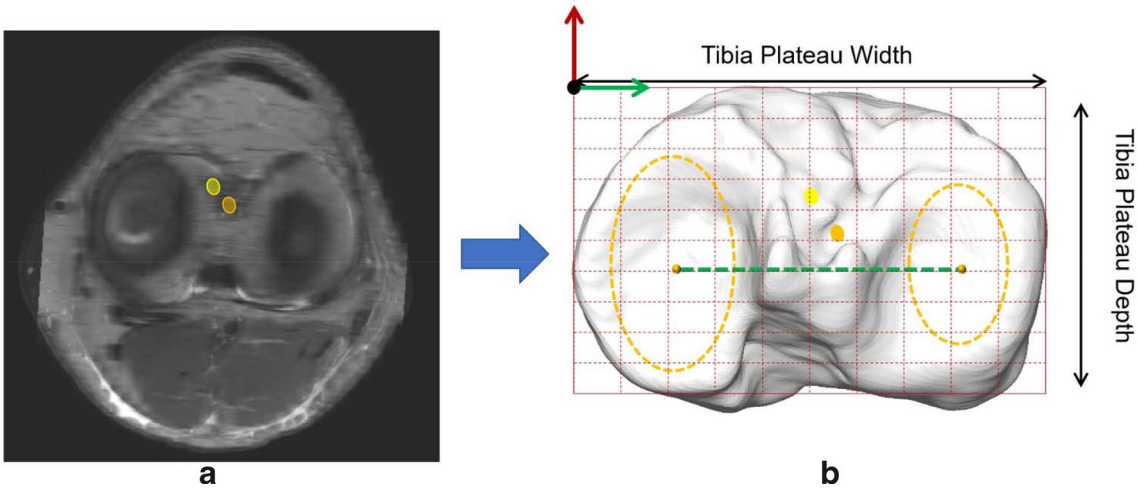

Fig. 2 Left knee with an intact ACL demonstrating the ACL bundle insertion. **a** High-resolution volumetric MR data were created after merging sagittal and coronal MR stacks. The tibial insertion of the AM and PL-bundles is marked with a yellow and orange ellipses, respectively. The origin of the AM and PL-bundles is marked with an orange and yellow ellipses, respectively. **b** The three-dimensional surface model of the proximal tibia with an anatomical coordinate system was reconstructed. The origin of the coordinate system is shown with a black circle, and the medial/lateral axis, connecting the center of the best-fitted ellipses on the articular surface of the medial and lateral tibial plateau, is shown with a green line. The anterior/posterior axis is labeled with a red arrow. Within the best-fitted plane, a bounding box was defined by the depth and width of the tibial plateau. The origin of the tACS was then moved to the most anterior and medial point of the bounding box

The *anterior–posterior* (*A/P*) axis of the fACS was established by creating the best-fitted cylinder of the femoral shaft and then taking the cross product of the central cylinder axis with the M/L axis. The *distal–proximal* (*D/P*) axis of the fACS was defined by the cross product of the M/L axis with the A/P axis. The origins of the fACS was defined as the midpoint of the intersections of the M/L axis with the most medial and the most lateral points of the distal femur,

respectively [37]. The commonly used quadrat method [1] was applied to compare the results of the present study with the existing literature. In this method, a 4 × 4 grid was applied to the medial aspect of the lateral femoral condyle. The anterior border of the grid was the Blumensaat line, whereas the posterior border was defined by a line drawn to the posterior edge of the lateral condyle parallel to the Blumensaat line. The proximal and distal borders were formed by two lines perpendicular to the Blumensaat line originating from the proximal and distal bony borders of the lateral femoral condyle (Fig. 3).

The anatomical coordinate system of the proximal tibia (tACS) was reconstructed following a previously established method [7]. In summary, two ellipses were best fitted to the articular surface of the medial and lateral tibial plateau using a Gauss–Newton nonlinear least square algorithm (Fig. 2b). The line connecting the centers of the best-fitted ellipses formed the mediolateral (M/L) axis of the tACS and the midpoint of the tibia center. The cross product of the M/L axis and the proximal tibial long axis formed the anteroposterior (A/P) axis of the tibia. The cross product of the M/L and A/P axes formed the proximal/distal (P/D) axis. A plane was then best fitted to the surface of the tibial plateau. The tibial plateau depth was defined as the A/P distance between the anterior border of the tibial plateau (where the plateau edge drops down to the shaft) and the posterior border of the tibial plateau. Similarly, the tibial plateau width was defined as the M/L distance between the medial and lateral border of the tibial plateau. Within the plane, a bounding box was defined by the depth and width of the tibial plateau. The origin of the tACS was then moved to the most anterior and medial point of the bounding box (Fig. 2b).

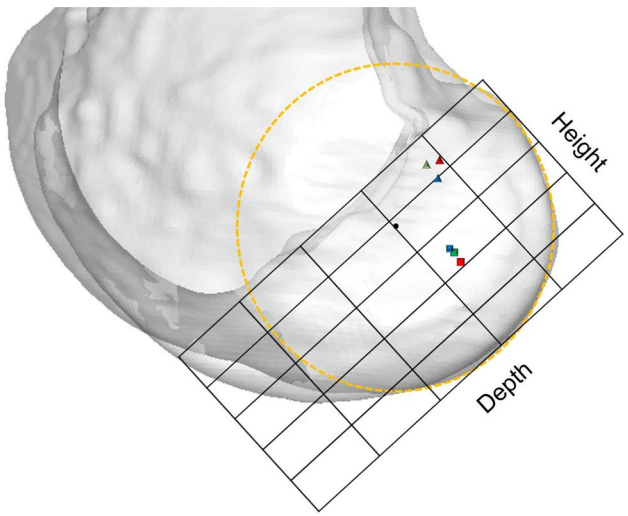

Fig. 3 Left distal femur demonstrating the average normalized femoral origin of the AM-bundle in ACL-intact (green triangle) and ACL-rupture knees (red triangle) and the PL-bundle in ACL-intact (green square) and ACL-rupture knees (red square) is demonstrated. The average location of the AM-bundle (blue triangle) and PL-bundle (blue square), as reported in the literature using the quadrat method [1], is also demonstrated

Repeatability analysis

Manual digitization was involved for the determination of the origin and insertions of the ACL bundles. Therefore, intraobserver and interobserver reliabilities of the measurements were evaluated with two independent blinded observers using single-measure intraclass correlation coefficients (ICC) with a two-way random-effects model for absolute agreement in all patients. The intraobserver ICC and interobserver ICC ranged from 0.85 to 0.99 (95% confidence interval 75–100%) for all the measurements.

Statistical analysis

A post hoc power analysis was performed to estimate the statistical power $(1-\beta)$, with medium effect size and $a=0.05$ using free statistical power analysis software (G*Power version 3.1; Franz Faul, Universität Kiel, Germany). The statistical power for detecting a difference between the ACL-footprint location in ACL-rupture and ACL-intact patients with 90 subjects in each group was 92%. Descriptive statistics used the average value, standard deviation, and range to describe all the continuous variables, whereas frequencies and percentages were applied to present the discrete data. All parameters were tested with the Kolmogorov–Smirnov test for normality. When the criteria for normality were met, a two-tailed *t* test was used. Otherwise, the Wilcoxon signed-rank test was applied. All statistical analyses were performed using SPSS version 23 software (SPSS Inc., Chicago, Illinois).

Results

Femoral AM-bundle origin

A statistically significant difference ($p<0.01$) in the average A/P location of the AM-bundle origin was found between the ACL-rupture (-4.8 ± 1.8 mm) and control (-3.5 ± 1.9 mm) groups. The normalized A/P femoral ACL-footprint location was located at an average of $24.5\pm9.0\%$ and $17.5\pm9.1\%$ posterior to the FEA of the knee in the ACL-rupture and control groups, respectively ($p<0.01$) (Fig. 3). No significant difference (*n.s.*) in the average or normalized P/D location of the AM-bundle origin was found between the ACL-rupture and control groups (Fig. 3; Table 1).

Table 1 Attachment location of AM-bundle and PL-bundle origin in femoral and tibial part between ACL-rupture and ACL-intact knees

	ACL-rupture		ACL-intact		*p* value	
	A/P	P/D	A/P	P/D	A/P	P/D
Femoral AM-bundle origin						
Average location (mm)	−4.8 ± 1.8	8.9 ± 1.8	−3.5 ± 1.9	8.3 ± 2.0	< 0.01	n.s
Normalized location (%)	24.5 ± 9.0% posterior	45.5 ± 10.5% proximal	17.5 ± 9.1% posterior	42.3 ± 10.5% proximal	< 0.01	n.s
Femoral PL-bundle origin						
Average location (mm)	−6.9 ± 2.4	−4.5 ± 2.1	−6.4 ± 2.4	−3.1 ± 1.8	n.s	< 0.01
Normalized location (%)	35.5 ± 12.5% posterior	22.4 ± 10.3% distal	32.1 ± 11.1% posterior	16.3 ± 9.4% distal	n.s	< 0.01
	A/P	M/L	A/P	M/L	A/P	M/L
Tibial AM-bundle insertion						
Average location (mm)	15.6 ± 2.6	37.1 ± 3.8	15.7 ± 3.2	35.6 ± 4.3	n.s	n.s
Normalized location (%)	34.3 ± 4.6	50.7 ± 3.5	34.4 ± 6.6	48.1 ± 4.6	n.s	n.s
Tibial PL-bundle insertion						
Average location (mm)	21.5 ± 2.5	41.8 ± 4.0	19.3 ± 2.7	42.1 ± 4.8	< 0.01	n.s
Normalized location (%)	47.5 ± 4.1	56.9 ± 3.4	42.7 ± 5.4	57.1 ± 4.8	< 0.01	n.s

Normalized location of bundle origin in femoral side was presented relative to the FEA position of the knee. Depth and width of the tibial plateau were used to normalize the location of bundle insertion in tibial side

A/P anterior (+)/posterior (−), *P/D* proximal (+)/distal (−), *M/L* medial (−)/lateral (+), *n.s.* no significant difference

Femoral PL-bundle origin

No significant difference (*n.s.*) in the average or normalized A/P location of the PL-bundle origin was found between the ACL-rupture and control groups. (Fig. 3; Table 1). A statistically significant difference ($p < 0.01$) in the average P/D location of the femoral ACL footprint was observed between the ACL-rupture (−4.5 ± 2.1 mm) and control (−3.1 ± 1.8 mm) groups. The normalized P/D femoral ACL-footprint locations were located at an average of 22.4 ± 10.3% and 16.3 ± 9.4% distal to the FEA of the knee in the ACL-rupture and control groups, respectively ($p < 0.01$) (Fig. 3; Table 1).

Tibial AM-bundle insertion

No significant difference (*n.s.*) in the average or normalized A/P location of the AM-bundle insertion was found between the ACL-rupture and control groups (Fig. 4; Table 1). No significant difference (*n.s.*) in the average or normalized M/L location of the AM-bundle insertion was found between the ACL-rupture and control groups (Fig. 4; Table 1).

Tibial PL-bundle insertion

A statistically significant difference ($p < 0.01$) in the average A/P location of the PL-bundle insertion was found between ACL-rupture (21.5 ± 2.5 mm) and control (19.3 ± 2.7 mm) groups. The normalized A/P location of the tibial footprint was found at an average of 47.5 ± 4.1% and 42.7 ± 5.4% of the tibial plateau depth in ACL-rupture and control groups, respectively ($p < 0.01$) (Fig. 4). No significant difference (*n.s.*) in the average or normalized M/L location of the PL-bundle insertion was observed between ACL-rupture and control groups (Fig. 4; Table 1).

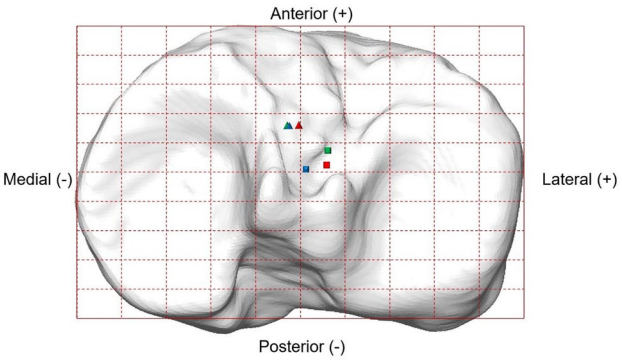

Fig. 4 Left proximal tibia demonstrating the average tibial insertion of the AM-bundle in ACL-intact (green triangle) and ACL-rupture patients (red triangle), and the average tibial insertion of the PL-bundle in ACL-intact (green square) and ACL-rupture patients (red square). The average location of the AM-bundle (blue triangle) and PL-bundle (blue square), as reported in the literature, is also demonstrated

Discussion

The most important finding of the present study was that the femoral origin of the AM-bundle is located more posteriorly in the same P/D direction, whereas the PL-bundle origin was found more distally in approximately the same A/P direction in ACL-rupture compared to ACL-intact knees. No significant difference was observed in the AM-bundle tibial insertion between groups, whereas the PL-bundle insertion was located more posteriorly in approximately the same M/L direction in ACL-rupture knees.

Several studies reported the femoral origin of the ACL bundles in ACL-intact knees with inconsistent results. Specifically, ten anatomical studies on a total of 191 human cadaveric knees reported the femoral origin of the ACL bundles (Table 2). The weighted average origin of the AM-bundle was 24.6% (range 15.0–33.9%) in the deep/shallow (D/S) direction and 20.5% (range 14.2–33.2%) in the high/low (H/L) direction, whereas the weighted average origin of the PL-bundle was 33.1% (range 27.0–40.6%) in the D/S direction and 48.7% (range 41.1–56.4%) in the H/L direction. In the present study, the femoral origin of the AM-bundle was located more proximally than the values reported in the literature, at an average of 24% in the P/D and 11% in the H/L direction, whereas the PL-bundle origin was found at the same location as reported in the literature in ACL-intact knees (Fig. 3). In ACL-rupture knees, the femoral origin of the AM-bundle was also located more proximally than the weighted average reported in the literature and more posteriorly than the AM-bundle location of the ACL-intact knees, at an average of 21% in the P/D direction and 14% in the H/L direction (Fig. 3). The average origin of the PL-bundle was slightly more posterior and more distal than in ACL-intact knees at 36% in the P/D and 55% in the H/L direction. The abovementioned difference might be attributed to the variable morphology of the distal femur between ACL-rupture and ACL-intact knees [27, 29, 31, 38]. Although the differences in the femoral attachment location of the ACL bundles might appear relatively small, several studies showed that even minor changes (3–5 mm) in femoral tunnel position could significantly affect the ACL graft length change patterns in knee motion [23, 42]. According to the in vivo ACL isometry distribution map on the femur reported by Kernkamp et al. [16], the more posterior femoral AM-bundle insertion and the more distal and posterior PL-bundle insertion that we found in the ACL-rupture knees were both farther away from the location of the most isometric ACL attachment than in the ACL-intact knees. Although the injury mechanism of the ACL-rupture knees in our study might be different from the functional movement studied by Kernkamp et al. it still implies that the variation in the femoral insertions of the ACL-rupture knees could result in a more anisometric elongation pattern prone to an ACL injury. Therefore, the results of the present study might constitute new insight into ACL bundle anatomy. Furthermore, since the femoral ACL tunnel guides during ACL reconstruction are based mostly on cadaveric studies in ACL-intact knees [3], they might not reproduce the native anatomy of the ACL-rupture knee. Further studies are required to investigate whether the contemporary femoral ACL guides could restore the anatomical ACL-footprint location in ACL-rupture knees.

To date, only six studies have described the tibial insertions of ACL bundles in studies performed on ACL-intact knees, with variable results (Table 3). The weighted average tibial insertion of the AM-bundle was 34.6% (range 25.0–41.0%) in

Table 2 Summary of the anatomic ACL femoral origin as reported in the literature ($n = 191$ knees) using the quadrat method [1]

Study	Subjects (*n*)	Study design	AM-bundle (%)		PL-bundle (%)	
			D/S	H/L	D/S	H/L
Colombet et al. [5]	7	Anatomical and lateral radiographs	26.4	25.3	32.3	47.6
Takahashi et al. [35]	31	Anatomical and lateral radiographs	31.9	26.9	39.8	53.2
Luites et al. [22]	35	Anatomical and 3D system	23.0	10.0	28.0	47.0
Zantop et al. [41]	20	Anatomical and lateral radiographs	18.5	22.3	29.3	53.6
Tsukada et al. [36]	36	Anatomical	25.9	17.8	34.8	41.1
Lorenz et al. [21]	12	Anatomical and 3D CT-scan	21.0	22.0	27.0	45.0
Iriuchishima et al. [13]	15	Anatomical and lateral radiographs	15.0	26.0	32.0	52.0
Forsythe et al. [10]	8	Anatomical and 3D CT-scan	21.7	33.2	35.1	55.3
Pietrini et al. [30]	12	Anatomical and lateral radiographs	21.6	14.2	28.9	42.3
Lee et al. [20]	15	Anatomical, lateral radiographs and CT-scan	33.9	25.6	40.6	56.4
Weighted average			24.6	20.5	33.1	48.7

3D three-dimensional, *ACL* anterior cruciate ligament, *AM* anteromedial, *CT* computed tomography, *D/S* deep-shallow, *H/L* high–low, *PL* posterolateral

Table 3 Summary of the anatomic ACL tibial insertion, as reported in the literature ($n = 106$ knees)

Study	Subjects (*n*)	Study design	AM-bundle (%)		PL-bundle (%)	
			A/P	M/L	A/P	M/L
Zantop et al. [41]	20	Anatomical and lateral radiographs	30	–	44.0	–
Tsukada et al. [36]	36	Anatomical	37.6	46.5	50.1	51.2
Lorenz et al. [21]	12	Anatomical and 3D CT-scan	41.0	52	52.0	50
Forsythe et al. [10]	8	Anatomical and 3D CT-scan	25.0	50.5	46.4	52.4
Iriuchishima et al. [13]	15	Anatomical and lateral radiographs	31.0	49	50	47.0
Lee et al. [20]	15	Anatomical, lateral radiographs and CT-scan	36.9	47.1	43.1	53.5
Weighted average			34.6	48.2	47.9	50.8

3D three-dimensional, *ACL* anterior cruciate ligament, *AM* anteromedial, *A/P* anteroposterior, *CT* computed tomography, *M/L* mediolateral, *PL* posterolateral

the A/P direction and 48.2% (range 47.1–50.5%) in the M/L direction, whereas the weighted average origin of the PL-bundle was 47.9% (range 43.1–52.0%) in the A/P direction and 50.8% (range 47.0–53.5%) in the M/L direction. In the present study, the tibial insertion of the AM-bundle was located at approximately the same weighted average location as reported in the literature, whereas the PL-bundle insertion was located approximately 5% more anterolaterally in ACL-intact knees (Fig. 4). In ACL-rupture knees, the tibial insertion of the AM-bundle was located at approximately the same location as in the ACL-intact knees, and the weighted average reported in the literature (Fig. 4). However, the average insertion of the PL-bundle in ACL-rupture knees was located approximately 5% more posteriorly than in ACL-intact knees and approximately 5% more laterally than the weighted average reported in the literature.

The present study should be interpreted with caution in the light of its potential limitations, which are mostly inherent to the MRI identification of ACL attachments. Although the gold standard technique is cadaveric dissection with histologic analysis, it is nearly impossible to preselect cadaveric knees with an ACL rupture, owing to the absence of the cadaver's medical history. However, due to the high-quality MRI images obtained after combining the sagittal- and coronal-plane images, the ACL bundle attachments were visible and distinct in all the patients. Furthermore, all the subjects in the present study were Caucasians. Therefore, the results of the present study might not reflect the ACL bundles' anatomy of the African-American or Asian population, as ethnic-specific anatomical variations of the knee have been reported [18].

Conclusion

The current study investigated the three-dimensional topographic anatomy of the ACL bundle in ACL-rupture and ACL-intact knees. The femoral origin of the AM-bundle was located more posteriorly in approximately the same P/D direction, whereas the PL-bundle origin was found more distally in approximately the same A/P direction in ACL-rupture knees relative to ACL-intact knees. No significant difference was observed in the AM-bundle tibial insertion between groups, whereas the PL-bundle tibial insertion was located more posteriorly in ACL-rupture knees. The results of the present study might help surgeons who perform anatomical double-bundle reconstruction surgery.

Author contributions DD: substantial contributions to research design, the acquisition, analysis, and interpretation of data, drafting the paper. DZ: substantial contributions to research design, acquisition, analysis and interpretation of data. ZW: substantial contributions to research design, acquisition, analysis and interpretation of data. NH: Critical revision and approval of the final version. T-YT: substantial contributions to research design, acquisition, analysis, and interpretation of data. Critical review and approval of the final version.

Funding This project was sponsored by the National Natural Science Foundation of China (31771017, 31972924), the Science and Technology Commission of Shanghai Municipality (16441908700), the Innovation Research Plan supported by Shanghai Municipal Education Commission (ZXWF082101), the National Key R&D Program of China (2017YFC0110700, 2018YFF0300504, and 2019YFC0120600), the Natural Science Foundation of Shanghai (18ZR1428600), and the Interdisciplinary Program of Shanghai Jiao Tong University (ZH2018QNA06, YG2017MS09).

Availability of data and material All data generated or analysed during this study are included in this published article.

Compliance with ethical standards

Conflict of interest The authors of this manuscript have nothing to disclose that would bias our work.

Ethical approval Ethikkommission Nordwest- und Zentralschweiz: 2018-01410.

Code availability AMIRA 6.5, FEI SVG, Thermo Fisher Scientific, Hillsboro, Oregon, USA; SPSS Inc., Chicago, Illinois; MATLAB, MathWorks, Natick, MA, USA.

References

1. Bernard M, Hertel P, Hornung H, Cierpinski T (1997) Femoral insertion of the ACL. Radiographic quadrant method. Am J Knee Surg 10:14–21
2. Beynnon BD, Hall JS, Sturnick DR, DeSarno MJ, Gardner-Morse M, Tourville TW et al (2014) Increased slope of the lateral tibial plateau subchondral bone is associated with greater risk of noncontact ACL injury in females but not in males: a prospective cohort study with a nested, matched case-control analysis. Am J Knee Surg 42:1039–1048
3. Burnham JM, Malempati CS, Carpiaux A, Ireland ML, Johnson DL (2017) Anatomic femoral and tibial tunnel placement during anterior cruciate ligament reconstruction: anteromedial portal all-inside and outside-in techniques. Arthrosc Tech 6:e275–e282
4. Cohen SB, VanBeek C, Starman JS, Armfield D, Irrgang JJ, Fu FH (2009) MRI measurement of the 2 bundles of the normal anterior cruciate ligament. Orthopedics 32:9–16
5. Colombet P, Robinson J, Christel P, Franceschi J-P, Djian P, Bellier G et al (2006) Morphology of anterior cruciate ligament attachments for anatomic reconstruction: a cadaveric dissection and radiographic study. Arthroscopy 22:984–992
6. Daggett M, Ockuly AC, Cullen M, Busch K, Lutz C, Imbert P et al (2016) Femoral origin of the anterolateral ligament: an anatomic analysis. Arthroscopy 32:835–841
7. Defrate LE, Papannagari R, Gill TJ, Moses JM, Pathare NP, Li G (2006) The 6 degrees of freedom kinematics of the knee after anterior cruciate ligament deficiency: an in vivo imaging analysis. Am J Sports Med 34:1240–1246
8. Dimitriou D, Wang Z, Zou D, Tsai TY, Helmy N (2019) The femoral footprint position of the anterior cruciate ligament might be a predisposing factor to a noncontact anterior cruciate ligament rupture. Am J Sports Med 47:3365–3372
9. Eckhoff D, Hogan C, DiMatteo L, Robinson M, Bach J (2007) Difference between the epicondylar and cylindrical axis of the knee. Clin Orthop Relat Res 461:238–244
10. Forsythe B, Kopf S, Wong AK, Martins CA, Anderst W, Tashman S et al (2010) The location of femoral and tibial tunnels in anatomic double-bundle anterior cruciate ligament reconstruction analyzed by three-dimensional computed tomography models. J Bone Jt Surg Am 92:1418–1426
11. Hodel S, Kabelitz M, Tondelli T, Vlachopoulos L, Sutter R, Fucentese SF (2019) Introducing the lateral femoral condyle index as a risk factor for anterior cruciate ligament injury. Am J Sports Med 47:2420–2426
12. Hollister AM, Jatana S, Singh AK, Sullivan WW, Lupichuk AG (1993) The axes of rotation of the knee. Clin Orthop Relat Res 290:259–268
13. Iriuchishima T, Ingham SJ, Tajima G, Horaguchi T, Saito A, Tokuhashi Y et al (2010) Evaluation of the tunnel placement in the anatomical double-bundle ACL reconstruction: a cadaver study. Knee Surg Sports Traumatol Arthrosc 18:1226–1231
14. Järvelä T (2007) Double-bundle versus single-bundle anterior cruciate ligament reconstruction: a prospective, randomize clinical study. Knee Surg Sports Traumatol Arthrosc 15:500–507
15. Kennedy MI, Claes S, Fuso FAF, Williams BT, Goldsmith MT, Turnbull TL et al (2015) The anterolateral ligament: an anatomic, radiographic, and biomechanical analysis. Am J Sports Med 43:1606–1615
16. Kernkamp WA, Varady NH, Li JS, Tsai TY, Asnis PD, van Arkel ERA et al (2018) An in vivo prediction of anisometry and strain in anterior cruciate ligament reconstruction—a combined magnetic resonance and dual fluoroscopic imaging analysis. Arthroscopy 34:1094–1103
17. Kilinc BE, Kara A, Oc Y, Celik H, Camur S, Bilgin E et al (2016) Transtibial vs anatomical single bundle technique for anterior cruciate ligament reconstruction: a retrospective cohort study. Int J Surg 29:62–69
18. Kim TK, Phillips M, Bhandari M, Watson J, Malhotra R (2017) What differences in morphologic features of the knee exist among patients of various races? a systematic review. Clin Orthop Relat Res 475:170–182
19. Kopf S, Forsythe B, Wong AK, Tashman S, Anderst W, Irrgang JJ et al (2010) Nonanatomic tunnel position in traditional transtibial single-bundle anterior cruciate ligament reconstruction evaluated by three-dimensional computed tomography. J Bone Jt Surg Am 92:1427–1431
20. Lee JK, Lee S, Seong SC, Lee MC (2015) Anatomy of the anterior cruciate ligament insertion sites: comparison of plain radiography and three-dimensional computed tomographic imaging to anatomic dissection. Knee Surg Sports Traumatol Arthrosc 23:2297–2305
21. Lorenz S, Elser F, Mitterer M, Obst T, Imhoff AB (2009) Radiologic evaluation of the insertion sites of the 2 functional bundles of the anterior cruciate ligament using 3-dimensional computed tomography. Am J Sports Med 37:2368–2376
22. Luites JW, Wymenga AB, Blankevoort L, Kooloos JG (2007) Description of the attachment geometry of the anteromedial and posterolateral bundles of the ACL from arthroscopic perspective for anatomical tunnel placement. Knee Surg Sports Traumatol Arthrosc 15:1422–1431
23. Markolf KL, Hame S, Hunter DM, Oakes DA, Zoric B, Gause P et al (2002) Effects of femoral tunnel placement on knee laxity and forces in an anterior cruciate ligament graft. J Orthop Res 20:1016–1024
24. McLean SG, Oh YK, Palmer ML, Lucey SM, Lucarelli DG, Ashton-Miller JA et al (2011) The relationship between anterior tibial acceleration, tibial slope, and ACL strain during a simulated jump landing task. J Bone Jt Surg Am 93:1310–1317
25. Miranda DL, Rainbow MJ, Leventhal EL, Crisco JJ, Fleming BC (2010) Automatic determination of anatomical coordinate systems for three-dimensional bone models of the isolated human knee. J Biomech 43:1623–1626
26. Muneta T, Koga H, Mochizuki T, Ju Y-J, Hara K, Nimura A et al (2007) A prospective randomized study of 4-strand semitendinosus tendon anterior cruciate ligament reconstruction comparing single-bundle and double-bundle techniques. Arthroscopy 23:618–628
27. Park JS, Nam DC, Kim DH, Kim HK, Hwang SC (2012) Measurement of knee morphometrics using MRI: a comparative study between ACL-injured and non-injured knees. Knee Surg Relat Res 24:180
28. Petersen W, Tretow H, Weimann A, Herbort M, Fu FH, Raschke M et al (2007) Biomechanical evaluation of two techniques for double-bundle anterior cruciate ligament reconstruction: one tibial tunnel versus two tibial tunnels. Am J Sports Med 35:228–234
29. Pfeiffer TR, Burnham JM, Hughes JD, Kanakamedala AC, Herbst E, Popchak A et al (2018) An increased lateral femoral condyle ratio is a risk factor for anterior cruciate ligament injury. J Bone Jt Surg Am 100:857–864
30. Pietrini SD, Ziegler CG, Anderson CJ, Wijdicks CA, Westerhaus BD, Johansen S et al (2011) Radiographic landmarks for tunnel positioning in double-bundle ACL reconstructions. Knee Surg Sports Traumatol Arthrosc 19:792–800

31. Simon R, Everhart J, Nagaraja H, Chaudhari A (2010) A case-control study of anterior cruciate ligament volume, tibial plateau slopes and intercondylar notch dimensions in ACL-injured knees. J Biomech 43:1702–1707
32. Sturnick DR, Argentieri EC, Vacek PM, DeSarno MJ, Gardner-Morse MG, Tourville TW et al (2014) A decreased volume of the medial tibial spine is associated with an increased risk of suffering an anterior cruciate ligament injury for males but not females. J Orthop Res 32:1451–1457
33. Sturnick DR, Van Gorder R, Vacek PM, DeSarno MJ, Gardner-Morse MG, Tourville TW et al (2014) Tibial articular cartilage and meniscus geometries combine to influence female risk of anterior cruciate ligament injury. J Orthop Res 32:1487–1494
34. Suomalainen P, Järvelä T, Paakkala A, Kannus P, Järvinen M (2012) Double-bundle versus single-bundle anterior cruciate ligament reconstruction: a prospective randomized study with 5-year results. Am J Sports Med 40:1511–1518
35. Takahashi M, Doi M, Abe M, Suzuki D, Nagano A (2006) Anatomical study of the femoral and tibial insertions of the anteromedial and posterolateral bundles of human anterior cruciate ligament. Am J Sports Med 34:787–792
36. Tsukada H, Ishibashi Y, Tsuda E, Fukuda A, Toh S (2008) Anatomical analysis of the anterior cruciate ligament femoral and tibial footprints. J Orthop Sci 13:122–129
37. von Eisenhart-Rothe R, Bringmann C, Siebert M, Reiser M, Englmeier KH, Eckstein F et al (2004) Femoro-tibial and menisco-tibial translation patterns in patients with unilateral anterior cruciate ligament deficiency–a potential cause of secondary meniscal tears. J Orthop Res 22:275–282
38. Whitney DC, Sturnick DR, Vacek PM, DeSarno MJ, Gardner-Morse M, Tourville TW et al (2014) Relationship between the risk of suffering a first-time noncontact ACL injury and geometry of the femoral notch and ACL: a prospective cohort study with a nested case-control analysis. Am J Sports Med 42:1796–1805
39. Wu C, Noorani S, Vercillo F, Woo S (2009) Tension patterns of the anteromedial and posterolateral grafts in a double-bundle anterior cruciate ligament reconstruction. J Orthop Res 27:879–884
40. Yagi M, Wong EK, Kanamori A, Debski RE, Fu FH, Woo SL (2002) Biomechanical analysis of an anatomic anterior cruciate ligament reconstruction. Am J Sports Med 30:660–666
41. Zantop T, Wellmann M, Fu FH, Petersen W (2008) Tunnel positioning of anteromedial and posterolateral bundles in anatomic anterior cruciate ligament reconstruction: anatomic and radiographic findings. Am J Sports Med 36:65–72
42. Zavras TD, Race A, Amis AA (2005) The effect of femoral attachment location on anterior cruciate ligament reconstruction: graft tension patterns and restoration of normal anterior-posterior laxity patterns. Knee Surg Sports Traumatol Arthrosc 13:92–100